Task-Oriented Optimal Grasping by Multifingered Robot Hands

ZEXIANG LI AND S. SHANKAR SASTRY, MEMBER, IEEE

Abstract—**The problem of optimal grasping of an object by a multifingered robot hand is discussed. Using screw theory and elementary differential geometry, the concept of a grasp is axiomated and its stability characterized. Three quality measures for evaluating a grasp are then proposed. The last quality measure is task oriented and needs the development of a procedure for modeling tasks as ellipsoids in the wrench space of the object. Numerical computations of these quality measures and the selection of an optimal grasp are addressed in detail. Several examples are given using these quality measures to show that they are consistent with measurements yielded by our experiments on grasping.**

I. Introduction

THE RISING interest in dextrous multifingered robot hands stems not only from a desire to increase the flexibility of the current generation industrial robot systems but also from a hope to improve prosthetic devices for humans that have either partially or completely lost their limb control [23]. In most industry applications the advantages of multifingered dextrous robot hands over the existing two-fingered parallel-jaw grippers are apparent since stacking an array of special-purpose grippers as proposed in [6] is both cumbersome and cost ineffective. The versatility of a human hand demonstrates a good example of using a multifingered dextrous hand instead of a simple two-fingered hand.

One of the most fundamental questions arising from the study of multifingered robot hands is the determination of an appropriate grasp: namely, given an object together with a task to be performed, what is the optimal grasp of the object so that the task can be executed efficiently? What dictates the choice of a grasp: stability, shape of the object, or the task requirement?

The determination of a stable grasp was extensively studied in [3]–[10], [19], and [21], using screw theory [5], [7], a potential function method [3], and a goal function method [9], etc. Using these approaches various stability criteria for a grasp have been proposed; e.g., in [5] and [7] it was concluded that a grasp was stable if and only if the grasp matrix was full row rank, and in [3] that a grasp was stable if the potential function was minimized at the grasping configuration. The author of [5] also considered the effect of unisense forces on the choice of a stable grasp, and the authors of [6]–[9] extended the work of [5] to include finite frictional forces. From human grasping experience, however, we observe that a stability criterion alone is not sufficient to characterize a grasp. The author in [6], after examining a variety of human grasps, concluded that the choice of a grasp was dictated less by the size and shape of the object than by the tasks to be performed with the object; the stability condition was only a necessary condition for a *good* grasp. A good grasp should be task oriented.

Undoubtedly, in designing a dextrous robot hand it is extremely important to know how to choose a grasp that is optimal with respect to the task to be performed. While the selection of a task-oriented optimal grasp is very easy for a human hand, it is a complicated process for a robot hand. In this paper we develop several grasping quality measures that could be used to evaluate a grasp for optimal selection of a grasp. A brief outline of the paper is as follows.

In Section II we axiomatize and formalize using screw theory and some elementary differential geometry in the concept of a grasp by a multifingered robot hand. The definitions are broad enough to cover both unisense and finite friction force contacts for a large number of commonly encountered contacts. Using this formalism we study and characterize the stability of a grasp.

In Section III, for different tasks we give three different quality measures for grasping: a min–max, or a worst case quality measure δ, a volumetric measure ν, and finally, the task-oriented measure μ. The development of the task-oriented measure μ requires the modeling of tasks. We have developed software to perform numerical computations of these quality measures, and a few sample applications of this software are presented in the text of the paper. Furthermore, we discuss the calculation of the optimal grasp (that optimizes μ, ν, or δ). Finally, we make some comments on grasping constraints imposed by oddly shaped objects, fine manipulation, and dynamic questions in manipulation. In Section IV we collect some suggestions for future work.

II. Rigid Body Motions and Grasping Structures

The following development of notation for rigid body motions and grasping structures is standard in the literature; see, for example, [5], [7], [12], and [27]. We review it here in compact form to fix notation.

A. Rigid Body Motions

Consider a rigid body $\boldsymbol{B}$ in R^3 (see Fig. 1). Let $\boldsymbol{X}$–$\boldsymbol{Y}$–$\boldsymbol{Z}$ be an arbitrarily chosen inertial frame and $\boldsymbol{x}$–$\boldsymbol{y}$–$\boldsymbol{z}$ be a coordinate

Manuscript received June 13, 1986; revised January 12, 1987. This work was supported in part by National Science Foundation PYI Grant DMC 8451129. This paper was presented in part at the IEEE International Conference on Robotics and Automation, Raleigh, NC, March 30–April 3, 1987.

The authors are with the Electronics Research Laboratory and Department of Electrical Engineering and Computer Sciences, University of California, Berkeley, CA 94720.

IEEE Log Number 8718071.

0882-4967/88/0200-0032$01.00

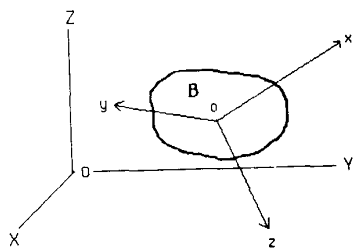

Fig. 1. Rigid body in R^3 space.

frame attached to the body. It is well-known [11], [22], [24] that the instantaneous configuration of the rigid body can be described by the orientation, and the position of the body frame x-y-z in terms of the inertial frame X-Y-Z. We define the configuration manifold M of the rigid body to be the space of configurations of the rigid body. Since three parameters are needed to specify an orientation and three more parameters for a position, the configuration manifold M is six dimensional. One of the standard ways to parametrize M is by using Euler angles and Cartesian coordinates [2], [22], but the computations involved are often messy. In the sequel, we will denote by $m \in M$ a nominal configuration of the rigid body and T_mM the tangent space to M at configuration m, which consists of all generalized velocities of the rigid body. A generalized velocity $\xi \in T_mM$ can be written as $\xi = (\omega, \nu)^t$, where $\omega \in R^3$, and $\nu \in R^3$ are called the angular and the linear velocity, respectively, of the rigid body. We also denote the set of generalized forces that can be exerted on the rigid body at configuration m by T_m^*M. T_m^*M is the cotangent space to M at m and is the space of all linear functionals of T_mM. An element $\eta \in T_m^*M$ is a combination of a force $f \in R^3$ and a moment $m \in R^3$ about the origin O of the inertial frame and can be written as $\eta = (f, m)^t$. In the literature, a generalized velocity ξ is also called a *twist* and a generalized force η a *wrench*. The work done per unit time by a generalized force η (a wrench) on a generalized velocity ξ (a twist) is given by

$$\langle \xi, \eta \rangle = \langle (\omega, \nu)(f, m) \rangle = \omega^t m + \nu^t f. \qquad (1)$$

Consider now two rigid bodies A and B in contact, and assume no energy losses or dissipation during the contact. Let $C^* \subset T_m^*M$ denote the set of contact wrenches that can be applied to B by A through the contact. The *principle of virtual work* states that to maintain the contact, the set of allowable twists $\xi \in T_mM$ of B relative to A must satisfy

$$\langle \xi, \eta \rangle = \langle (\omega, \nu), (f, m) \rangle = 0, \qquad \text{for all } \eta \in C^*. \qquad (2)$$

Contacts can be thought of as constraints on the motion of a rigid body. For a given set $C^* \subset T_m^*M$, we define a set $C \subset T_mM$ by

$$C = \{ \xi \in T_mM, \text{ such that } \langle \xi, \eta \rangle = 0, \text{ for all } \eta \in C^* \} \qquad (3)$$

which is called the annihilator of C^* in T_mM, and we have the following theorem.

Theorem 1 (Principle of Virtual Work): When a rigid body B is constrained such that the set of contact wrenches can be exerted on B is $C^* \subset T_m^*M$, the set of allowable twist motions of B is precisely the annihilator C of C^* in T_mM.

B. Grasping Structures

We shall be concerned in this paper mainly with three basic contact types: 1) a point contact without friction, 2) a point contact with friction, and 3) a soft finger contact. These contact types along with others are studied extensively in [5]–[7] and [9]. Denote by n_c the number of independent contact wrenches that can be exerted on a rigid body at the contact. We have n_c to be 1 for a point contact without friction, 3 for a point contact with friction, and 4 for a soft finger contact. For a more general kind of contact, such as the contact of a line with a plane, etc., the value of n_c may be found in [5, table 2-3]. It is important to remember that all of these contacts are idealization of true (complicated) contacts which involve a nonzero area.

A study of the following example will help in motivating the definition of a contact. We will use this example repeatedly in the paper.

Example 1: Consider a three-fingered robot hand contacting a cube as shown in Fig. 2. Assume that finger I is modeled as a point contact without friction, finger II a point contact with friction, and finger III a soft finger contact. With the body coordinate x-y-z shown as in the figure, let us obtain a matrix representation of each contact map represented as a map from the applied independent contact forces to the wrench space of the object.

Finger I: Define ψ_{c1} to be the map taking the normal finger force applied at finger I to the body wrenches (all torques are measured with respect to o):

$$\psi_{c1}: R^1 \to T_m^*M$$

$$\psi_{c1}(x) = \begin{bmatrix} f_1^1 \\ f_1^1 \times (p_1 - o) \end{bmatrix} x = \begin{bmatrix} 0 \\ 0 \\ 1 \\ -p_y^1 \\ p_x^1 \\ 0 \end{bmatrix} [x]. \qquad (4a)$$

Finger II: Define ψ_{c2} to be the map taking the three applied finger forces at finger II, namely, the normal force and two orthogonal friction forces, to the body wrench:

$$\psi_{c2}: R^3 \to T_m^*M$$

$$\psi_{c2}(x_1, x_2, x_3)$$

$$= \begin{bmatrix} f_1^2 & f_2^2 & f_3^2 \\ f_1^2 \times (p_2 - o) & f_2^2 \times (p_2 - o) & f_3^2 \times (p_2 - o) \end{bmatrix} \begin{bmatrix} x_1 \\ x_2 \\ x_3 \end{bmatrix}$$

$$= \begin{bmatrix} 1 & 0 & 0 \\ 0 & 1 & 0 \\ 0 & 0 & 1 \\ 0 & p_z^2 & -p_y^2 \\ -p_z^2 & 0 & p_x^2 \\ p_x^2 & -p_x^2 & 0 \end{bmatrix} \begin{bmatrix} x_1 \\ x_2 \\ x_3 \end{bmatrix}. \qquad (4b)$$

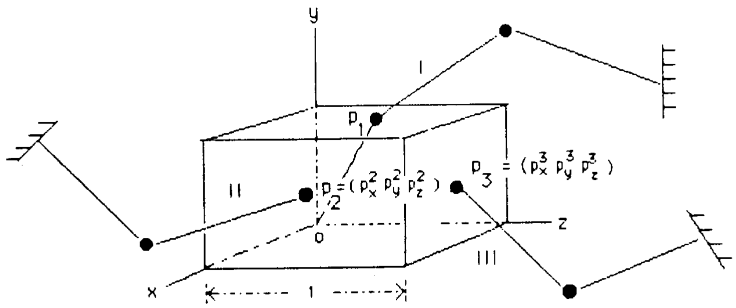

Fig. 2. Three-fingered robot hand contacts cube.

Finger III: Define ψ_{c3} to be the map taking the three applied finger forces and one normal torque at finger III to the body wrench:

$$\psi_{c3}: R^4 \rightarrow T_m^* M$$

$\psi_{c3}(x_1, x_2, x_3, x_4)$

$$= \begin{bmatrix} f_1^3 & f_2^3 & f_3^3 & 0 \\ f_1^3 \times (p_3 - o) & f_2^3 \times (p_3 - o) & f_3^3 \times (p_3 - o) & m_4^3 \end{bmatrix} \begin{bmatrix} x_1 \\ x_2 \\ x_3 \\ x_4 \end{bmatrix}$$

$$= \begin{bmatrix} 0 & 1 & 0 & 0 \\ 1 & 0 & 0 & 0 \\ 0 & 0 & 1 & 0 \\ p_z^3 & 0 & -p_y^3 & 0 \\ 0 & -p_z^3 & p_x^3 & 1 \\ -p_x^3 & p_x^3 & 0 & 0 \end{bmatrix} \begin{bmatrix} x_1 \\ x_2 \\ x_3 \\ x_4 \end{bmatrix}. \tag{4c}$$

Notice that f_1^i and m_4^i in the previous equations are the unit normals to the contact surface (i.e., surfaces of the rigid body) at the ith contact point. f_2^i and f_3^i are the unit tangent vectors to the contact surface, and they determine along with f_1^i an orthonormal basis at the ith contact point. Motivated by this and similar examples, we define a contact as follows.

Definition 1 (Contact)[1]*:* A contact on a rigid body in configuration m is a map

$$\psi_c: R^{n_c} \rightarrow T_m^* M \tag{5}$$

where n_c is the total number of independent contact wrenches that can be exerted on the rigid body at the contact and that depends on the structure of the contact alone.

Similarly, we define a grasp of a rigid body by a robot hand as a group of contacts. For this we assume the hand has k fingers, each finger contacts the object at one point (at the fingertip only), and each defines a contact map $\psi_{ci}: R^{n_i} \rightarrow T_m^* M$, for $i = \{1, \cdots, k\}$.

Definition 2 (Grasp): A grasp of a rigid body at configuration m by a robot hand with k fingers is a map

$$G: R^n \rightarrow T_m^* M, \qquad n = \sum_{i=1}^{i=k} n_i$$

given by

$$G(x_1, x_2, \cdots, x_n) = \psi_{c1}(x_1, \cdots, x_{n_1}) + \cdots + \psi_{ck}(x_{n-n_k}, \cdots, x_n). \tag{6}$$

Remark 1: Given a grasp configuration, we outline a procedure to obtain a matrix representation of the grasp map: a) Specify a body coordinate and obtain the coordinates of each contacting point. b) Determine the unit normal and the two orthogonal tangent vectors to the contacting surface at the contact point. c) Pick a torque origin in the body coordinates and construct for each contact map the contact matrix as in Example 1. d) Concatenate these contact matrices side by side into a big matrix. This is the grasp matrix for the particular choice of the body coordinates and the particular choice of the torque origin.

For example, the grasp map of Fig. 2 is obtained by adding the contact maps (4a)–(4c), i.e.,

$$G = \begin{bmatrix} f_1^1 & f_1^2 & f_2^2 & f_3^2 & f_1^3 & f_2^3 & f_3^3 & 0 \\ f_1^1 \times (p_1 - o) & f_1^2 \times (p_2 - o) & f_2^2 \times (p_2 - o) & f_3^2 \times (p_2 - o) & f_1^3 \times (p_3 - o) & f_2^3 \times (p_3 - o) & f_3^3 \times (p_3 - o) & m_4 \end{bmatrix}$$

$$= \begin{bmatrix} 0 & 1 & 0 & 0 & 0 & 1 & 0 & 0 \\ 0 & 0 & 1 & 0 & 1 & 0 & 0 & 0 \\ 1 & 0 & 0 & 1 & 0 & 0 & 1 & 0 \\ -p_y^1 & 0 & p_z^2 & -p_y^2 & p_z^3 & 0 & -p_y^3 & 0 \\ p_x^1 & -p_z^2 & 0 & p_x^2 & 0 & -p_z^3 & p_x^3 & 1 \\ 0 & p_x^2 & -p_x^2 & 0 & -p_x^3 & p_x^3 & 0 & 0 \end{bmatrix}. \tag{7}$$

[1] Such a definition was suggested to us by P. Jacobs [32] at Berkeley.

Remark 2: In obtaining a matrix representation of a grasp map, it is often convenient to get the finger contact wrenches relative to coordinate systems at the contacting points first and then transform these contacting wrenches to the body coordinate. This is done using a wrench transformation matrix (Kerr [7]), and a procedure for obtaining such a matrix, along with Example 1, is presented in [26].

C. Grasping under Unisense and Finite Frictional Forces

In Definition 1 (or 2) we have implicitly assumed bidirectional and infinite frictional forces by allowing the force domain of the contact map (or the grasp map) to range over the entire space R^{n_c} (or R^n). However, in reality two objects in contact cannot pull on each other, and sliding is frequently observed even between rough contacting surfaces. To handle unisense and finite frictional forces, we need to restrict the force domain of a contact map (or a grasp map) to an appropriate subset of R^{n_c} (or R^n). Consider again the example of Fig. 2; assuming Coulomb frictional models for each contact, we obtain the force domains of the contact map ψ_{ci}:

$$\psi_{c1}\colon K_1 = \{x \in R^1, \text{ such that } x \geq 0\}$$

$$\psi_{c2}\colon K_2 = \{x \in R^3, \text{ such that } x_1 \geq 0,\ x_2^2 + x_3^2 \leq \mu_1^2 x_1^2\}$$

$$\psi_{c3}\colon K_3 = \{x \in R^4 \text{ such that } x_1 \geq 0,\ x_2^2 + x_3^2 \leq \mu_2^2 x_1^2,\ |x_4| \leq \mu_t x_1\} \quad (8)$$

where the μ_i are the Coulomb friction coefficients of the respective contacting surfaces, and μ_t the torsional friction coefficient [7]. The force domain $\boldsymbol{K}$ of a grasp map is the product of each contact force domain K_1, K_2, and K_3 in the product space $R^1 \oplus R^3 \oplus R^4 = R^8$. The force domain of a contact map modeled by a Coulomb frictional law has a very nice property: convexity.

Proposition 1: The set K_i for $i = \{1, \cdots, 3\}$ in (8) is a convex cone.

Proof: It is straightforward using convex analysis; see, for example, [26].

Corollary 1: The product of convex cones is again a convex cone. Consequently, the force domain $\boldsymbol{K}$ of the grasp map (7) is a convex cone.

D. Stability of a Grasp and Body Coordinate Transformations

In applications, we are interested in characterizing the stability of a grasp. We say that a grasp is *stable* (or *statically stable*) if and only if it can balance disturbance forces in all directions.

Proposition 2: A grasp $\boldsymbol{G}$ defined in (6) is statically stable if and only if the associated grasp map is surjective.

Proof: Suppose that $\boldsymbol{G}$ is surjective; then for any disturbance wrench $\omega_d \in T_m^*M$, a finger force $x \in R^n$ exists such that

$$G(x) = \omega_d \quad (9)$$

i.e., the disturbance wrench is exactly balanced out by the contact wrench. The converse part follows from the definition.

Corollary 2: A grasp $\boldsymbol{G}$ with associated force domain $\boldsymbol{K} \subset R^n$ is (statically) stable if and only if the associated grasp map $\boldsymbol{G}$ restricted to $\boldsymbol{K}$ is surjective.

In the following discussions, the set $K \subset R^n$ always refers to the force domain of a grasp map $\boldsymbol{G}$; it is a convex cone in R^n and may be the entire space. When the set $\boldsymbol{K}$ equals R^n, the stability condition for a grasp $\boldsymbol{G}$ requires that the grasp matrix be of full row rank. When $\boldsymbol{K}$ is a proper subset of R^n, we define

$$B_1^n = \{x \in R^n,\ \|x\|_2^2 \leq 1\} \quad (10)$$

to be the unit ball of R^n and let O_ϵ denote an ϵ open ball at the origin of R^6 ($= T_m^*M$). We have the following.

Proposition 3: A grasp $\boldsymbol{G}$ with force domain $\boldsymbol{K}$ is stable if and only if there exists an ϵ-ball O_ϵ, $\epsilon > 0$, such that

$$O_\epsilon \subset G(K \cap B_1^n). \quad (11)$$

Proof: Suppose (11) is true; then for any $y \in T_m^*M$, $\alpha > 0$ exists such that $\|y\|/\alpha \leq \epsilon$. Let $\tilde{y} = y/\alpha$; then $\tilde{y} \in O_\epsilon$ and (11) implies existence of $\tilde{x} \in (\boldsymbol{K} \cap B_1^n)$ such that

$$G(\tilde{x}) = \tilde{y} = \frac{y}{\alpha} \quad \text{and} \quad G(\alpha\tilde{x}) = y.$$

However, the set $\boldsymbol{K}$ is a convex cone; therefore, $x = \alpha\tilde{x} \in \boldsymbol{K}$, and $G|_K$ is surjective.

Physically, a grasp with a restricted force domain is stable if disturbance forces can be balanced with finger forces from the defined force domain only. Proposition 3 relies on the convexity property of a force domain to provide an efficient method for a stability test. Modified algorithms of [15] can be used to perform the test, and further details about this issue are discussed in Section III-D.

Example 2: Consider again the grasp of Fig. 2, whose matrix representation is given in (7). Using a modification of the algorithms of [15], we found that, with all friction coefficients set to 1, $\boldsymbol{G}(\boldsymbol{K} \cap B_1^n)$ contained an open ball at the origin of radius 0.2. Therefore, by Proposition 3 the grasp $\boldsymbol{G}$ is stable.

In practice, when one constructs a grasp matrix there are no natural ways to choose body coordinates and a torque origin. Hence we need to consider the consequences of changing a body coordinate and changing a torque origin on the matrix representation of the grasp map. First, we see from previous examples that varying the body coordinate results in different grasp matrices, assuming the torque origin coincides with the origin of each body coordinate. It is well known [17] that a change of the body coordinate can be described by an element $\boldsymbol{T} = (\boldsymbol{A}, \boldsymbol{b})$ of SE(3), the group of proper rigid motions in R^3, where $\boldsymbol{A} \in$ SO(3) is a 3×3 orthogonal matrix with determinant $+1$, and $\boldsymbol{b} \in R^3$. Let the change of the body coordinate from x-y-z to x'-y'-z' be denoted by $\boldsymbol{T} = (\boldsymbol{A}, \boldsymbol{b}) \in$ SE(3); a point x in the old body coordinate is transformed to a point $\tilde{x}$ in the new body coordinate, according to

$$\tilde{x} = T(x) = Ax + b. \quad (12)$$

More generally, the matrix representation of the contact map (4c) is transformed under $\boldsymbol{T}$ to

$$\begin{aligned}\tilde{\psi}_{c3} &= \begin{bmatrix} Af_1^3 & Af_2^3 & Af_3^3 & 0 \\ Af_1^3 \times A(p_3-o) & Af_2^3 \times A(p_3-o) & Af_3^3 \times A(p_3-o) & Am_4^3 \end{bmatrix} \\ &= \begin{bmatrix} A & 0 \\ 0 & A \end{bmatrix} \begin{bmatrix} f_1^3 & f_2^3 & f_3^3 & 0 \\ f_1^3 \times (p_3-o) & f_2^3 \times (p_3-o) & f_3^3 \times (p_3-o) & m_4^3 \end{bmatrix} \\ &= \tilde{T}\psi_{c3} \end{aligned} \tag{13}$$

where $\tilde{T}$ is the diagonal matrix with A's on the diagonal. It then follows that the matrix representation of any grasp map under the body coordinate transformation $\boldsymbol{T}$ can be expressed as

$$\tilde{G} = \tilde{T}G. \tag{14}$$

We now consider changing the torque origin from "o" to a new point $\boldsymbol{b} = (b_1, b_2, b_3)$. We first define a skew symmetric matrix from $(b - o)$ by

$$A = \begin{bmatrix} 0 & -b_3 & b_2 \\ b_3 & 0 & -b_1 \\ -b_2 & b_1 & 0 \end{bmatrix};$$

then for any $f \in R^3$,

$$Af = (b-o) \times f = f \times (o-b), \tag{15}$$

and the new matrix representation of the grasp map is

$$\begin{aligned}\tilde{G} &= \begin{bmatrix} f_1^1 & f_2^1 & \cdots & 0 \\ f_1^1 \times (p_1-b) & f_2 \times (p_1-b) & \cdots & m_4^k \end{bmatrix} \\ &= \begin{bmatrix} f_1^1 & f_2^1 & \cdots & 0 \\ f_1^1 \times (p_1-o) + f_1^1 \times (o-b) & f_2^1 \times (p_1-o) + f_2^1 \times (o-b) & \cdots & m_4^k \end{bmatrix} \\ &= \begin{bmatrix} I & 0 \\ A & I \end{bmatrix} \begin{bmatrix} f_1^1 & f_2^1 & \cdots & 0 \\ f_1^1 \times (p_1-o) & f_2^1 \times (p_1-o) & \cdots & m_4^k \end{bmatrix} \\ &= \hat{T}_b G \end{aligned} \tag{16}$$

i.e., a change of the torque origin corresponds to multiply the original grasp matrix on the left by a nonsingular matrix $\hat{T}_b$.

Remark 3: $\tilde{T}$ is unitary, i.e., $\tilde{T}^t\tilde{T} = I$, but $\hat{T}_b$ is not. This is important since only a unitary matrix preserves norms.

Theorem 2: Stability properties of a grasp $\boldsymbol{G}$ are invariant under a body coordinate transformation and under a change of the torque origin.

Proof: From (14) or (16), $\tilde{T}$ or $\hat{T}_b$ is nonsingular and surjectivity of $\boldsymbol{G}$ is thus preserved.

III. Optimal Grasping Theory

We have studied the static stability of a grasp and defined a stable grasp in terms of its ability to reject disturbance forces. It is clear that as a basic requirement any choice of a grasp must satisfy the stability criterion. Hence we could narrow the set of all grasps of an object to a smaller set of stable grasps only. The need to select an optimal grasp among a set of stable grasps motivates the study of grasping quality measures. A quality measure for optimal grasping is like a partial ordering or a seminorm in a Euclidean space; it is used to evaluate the relative qualities of grasps of an object. As many ways exist to define a seminorm in a Euclidean space, many ways also exist to define a quality measure for optimal grasping. We propose three different grasping quality measures in this section: a minmax measure, a volumetric measure, and a task-oriented measure. The first two quality measures are similar to the manipulability measures defined by Yoshikawa [25] on the manipulator Jacobian matrices.

A. Quality Measure δ: Smallest Singular Value of $\boldsymbol{G}$

We first consider a matrix $\boldsymbol{G} \in R^{m \times n}$ with rank $\boldsymbol{r}$. The n nonnegative square roots σ_i of the eigenvalues of G^tG are called singular values of $\boldsymbol{G}$. When ordered according to

$$\sigma_1 \ge \sigma_2 \ge \cdots \sigma_r > 0 = \sigma_{r+1} = \cdots = \sigma_n,$$

the first r singular values are called positive and are given by the singular value decomposition of $\boldsymbol{G}$ [30]. A complete picture of the action of a matrix $\boldsymbol{G} \in R^{m \times n}$ is the image under $\boldsymbol{G}$ of the unit sphere of R^n. $\boldsymbol{G}$ maps the unit sphere of R^n onto an r-dimensional ellipsoid in the range space of $\boldsymbol{G}$. The lengths of the principal axes of the ellipsoid are the positive singular values of $\boldsymbol{G}$.

Now let $\boldsymbol{G}$ be the grasp matrix associated with the grasp map (6), where $\boldsymbol{m} = 6$. We define the quality $\delta(G)$ of the grasp $\boldsymbol{G}$ as

$$\delta(G) = \sigma_{\min}(G) \tag{17a}$$

where $\sigma_{min}(G)$ stands for the smallest singular value of the matrix $\boldsymbol{G}$. We say that $G_1 \ge G_2$ if and only if $\delta(G_1) \ge \delta(G_2)$.

We observe that $\delta(G)$ gives a worst case analysis of the grasp, and $\delta(G)$ is positive if and only if $\boldsymbol{G}$ is surjective. Hence the quality measure captures the stability property of a grasp.

Using this quality measure we will choose among a set of stable grasps one that maximizes the quality δ. Technical details for finding such a grasp are provided in Section III-E.

In (17a), we have implicitly assumed that the set K is the entire space R^n. In the general case we modify (17a) to

$$\delta(G) = \inf_{y \in R^6} \{\|y\| \text{ such that } y \notin G(B_1^n \cap K)\}. \tag{17b}$$

Namely, the quality measure $\delta(G)$ is the minimum distance of the complement set of $G(B_1^n \cap K)$ to the origin of R^6. Equation (17b) yields the smallest singular value of G when the set K is R^n itself. It is not difficult to see that the quality measure $\delta(\cdot)$ defined in (17a) or (17b) is invariant under a body coordinate transformation but *not invariant* under a change of the torque origin. Thus one should be very careful in selecting the torque origin to construct the grasp matrix.

B. Quality Measure ν: Volume in Wrench Space

While the quality measure δ has the desirable feature of both geometric and computational simplicity, it is not invariant under a change of the torque origin. Also, since it gives only a worst case analysis, it does not reflect the entire grasp. For example, two grasps G_1 and G_2, with singular values ($\sigma_1^1 \geq \cdots \geq \sigma_6^1$) and ($\sigma_1^2 \geq \cdots \geq \sigma_6^2$), respectively, with $\sigma_i^1 > \sigma_i^2$ for all i except for $i = 6$ where they are equal, would give the same grasp quality δ. To alleviate this drawback, we introduce a new quality measure $\nu(G)$, called the volume measure of G, defined by

$$\nu(G) = \int_{G(B_1^n \cap K)} d\nu \tag{18}$$

i.e., it is the volume in $T_m^* M$ of the set $G(B_1^n \cap K)$. Geometrically, G maps the set $B_1^n \cap K$ into a compact subset of R^6, and the geometric volume of the image is the volume measure of G. When the set K constitutes the entire space R^n, computation of (18) is especially simple, as given by the following.

Proposition 4: Let $\sigma_1, \sigma_2, \cdots, \sigma_6$ denote the set of singular values of a grasp matrix G. Then a $\beta > 0$ exists such that for the case $K = R^n$,

$$\nu(G) = \beta(\sigma_1 \cdot \sigma_2 \cdot \cdots \cdot \sigma_6). \tag{19}$$

Proof: Follows from the definition of singular values of a matrix.

The volume measure $\nu(\cdot)$ is uniform in all directions, i.e., all singular values are weighted equally. Furthermore, it is bi-invariant.

Theorem 3: The volume measure $\nu(\cdot)$ of (18) is invariant under both a body coordinate transformation and a change of the torque origin.

Proof: Since both $\tilde{T}$ and $\tilde{T}_b$ that represent the corresponding coordinate transformation and change of the torque origin are of determinant $+1$, the proof follows from the change of variable theorem in integration theory; see Boothby [17].

For a bi-invariant quality measure such as $\nu(\cdot)$, we can first construct the grasp matrix with respect to any coordinate frame and to any torque origin and evaluate the quality of the grasp. For another grasp we could as well evaluate its quality with respect to a new coordinate system and to a new torque origin and the results are comparable.

Nevertheless, undesirable features are also associated with the volume measure, it does not reflect stability of a grasp G. Namely, when the set K is an only proper subset of R^n, the set $G(B_1^n \cap K)$ may be a half-space in $T_m^* M$ but have nonzero volume measure. In this case, an unstable grasp might give a larger volume measure than a stable grasp. Consequently, to compare the qualities of two grasps, we have to first check their stability and then use (18). Section III-D presents numerical considerations regarding computation of $\nu(\cdot)$ in the general case.

Example 3: Consider the two grasps by a three-fingered hand to a hexagon in Fig. 3, with all finger contacts modeled as point contacts with friction and all friction coefficients set to 1. The geometry of the hexagon and details of each grasping configuration are shown in the figure. Along the lines of the previous discussion, we construct grasp matrices G_1 and G_2 (with "o" being the torque origin) for grasp configuration Fig. 3(a) and (b). The force domain of each grasp map is defined from the given assumptions, and the quality measures $\delta(\cdot)$ and $\nu(\cdot)$ of G_1 and G_2 are computed as (see Section III-D)

$$\delta(G_1) = 0.768 \qquad \delta(G_2) = 0.357$$
$$\nu(G_1) = 26.7 \qquad \nu(G_2) = 7.85.$$

Hence the grasp in Fig. 3(a) is a better grasp than the grasp in Fig. 3(b), and this is consistent with practical experience as the reader can readily verify.

C. Task-Oriented Quality Measure μ

The quality measures we have introduced are all unrelated to the tasks to be performed; consequently, they are useful only in a limited set of applications. Typical applications in this category include simple tasks, e.g., pick-and-place operations, waste disposal, etc., and object maneuvering in an *uncertain environment*. For more complicated applications, such as grasping a pencil to write, inserting a peg in a hole, and maneuvering an object in a *known environment,* it is unclear that using these quality measures will result in the optimal grasp for the task. More specifically, consider the example of pencil grasping shown in Fig. 5, where two grasping configurations are given. As an experienced person can readily tell, the grasp in Fig. 5(a) is a better choice than the grasp in Fig. 5(b) as far as the writing task is concerned. However, the latter grasp obviously gives higher grasping qualities δ and ν. This lack of generality associated with measures δ and ν indicates a need to incorporate the task requirement and the environment knowledge in the grasp quality measures. Namely, the choice of a grasp should also be based on its capability to generate body wrenches that are relevant to the task. Grasps that generate only body wrenches that are irrelevant to the task should be given low measures. A quality measure that takes account of the task requirement is

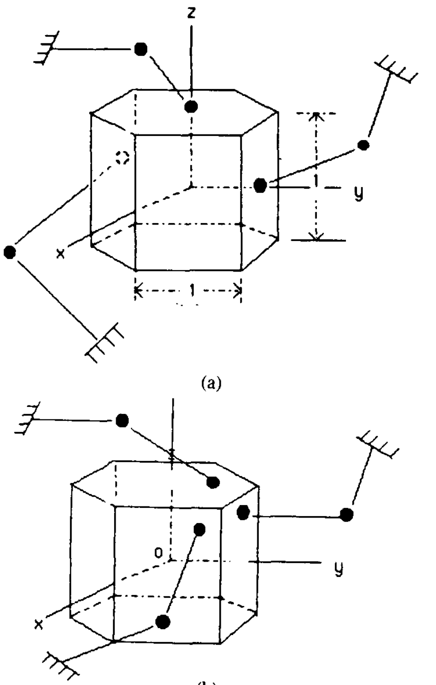

Fig. 3. Two grasp configurations to hexagon.

said to be task oriented, and the development of a task oriented quality measure is our aim in this section.

The development starts with a procedure to properly model the task and the working environment. Previous researchers [10] have done some work in this area, but none of their solutions are adequate for our purpose. Herein we present an approach to model tasks by ellipsoids in the wrench space (T_m^*M) of the object, called task ellipsoids. As we will see, modeling tasks by task ellipsoids is very natural and consistent with our experience with grasping.

1) Task Ellipsoids: We use the following examples to illustrate the procedure of modeling tasks and working environment by task ellipsoids.

Example 4: Consider the peg insertion task depicted in Fig. 4, where the robot grasps the workpiece and inserts it into the hole. To execute the task, a nominal trajectory is planned before the grasping action. The working environment and geometry of the workpiece is assumed known. After grasping the object the hand follows the planned trajectory until some misalignment of the peg or the hole causes the object to deviate from the nominal trajectory and collide with the environment.

With the body coordinate chosen as shown, we can see that the likehood of collision in each force direction of decreasing order would be $-f_y$, $\pm\tau_z$, $\pm\tau_x$, $\pm f_z$, $\pm f_x$, $\pm\tau_y$, $+f_y$. If we denote by $(r_i)_{i=1}^6$ the ratio of maximum expected collision forces in each force direction, we obtain a set A_β, parameterized by β, in the wrench space of the object:

$$A_\beta = \left\{ (f_x, \cdots, \tau_z) \in R^6, \quad \frac{(f_y+c_1)^2}{r_1^2} + \frac{\tau_z^2}{r_2^2} + \frac{\tau_x^2}{r_3^2} + \frac{(f_z-c_2)^2}{r_4^2} + \frac{f_x^2}{r_5^2} + \frac{\tau_y^2}{r_6^2} \le \beta^2 \right\} \quad (20)$$

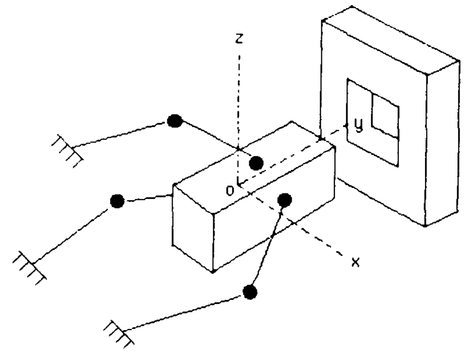

Fig. 4. Peg-in-hole task.

where the constant c_1 reflects the offset of maximum expected collision force in $+f_y$ and $-f_y$ directions, and c_2 reflects the gravitational force on the object. The set A_β is an ellipsoid in T_m^*M, centered at $(0, -c_1, c_2, 0, 0, 0)$, with principal axes given by each generalized force direction and axis lengths given by the ratio of maximum expected collision forces. The size of the ellipsoid is given by the parameter β, and intuitively, a good grasp should contain a large task ellipsoid in its image space.

By appropriately assigning a set of values to the constants (r_i, $i = 1, \cdots, 6$) and (c_i, $i = 1, 2$), we can decide on the shape of the task ellipsoid so that it meets the task requirement. In particular, the peg insertion task requires that ($r_i \ge r_j$) whenever ($j \ge i$) and c_1 be large when collisions in the $+f_y$ direction are unlikely. The effectiveness of the task ellipsoid in modeling the actual task can be improved as we accumulate more experience with the task and tasks of similar kinds.

Example 5: Consider the example of grasping a pencil to write (see Fig. 5). Human experience tells us that to execute the task efficiently, the grasp should provide 1) as much dexterity in the lead as possible and 2) sufficient normal forces at the pencil lead. With the body coordinate shown in the figure, the task specifications are translated into 1) a high torque requirement in the $\pm\tau_z$ and $\pm\tau_y$ directions, and 2) large normal contacting forces in the $+f_x$ direction. If we use $(r_i)_{i=1}^6$ to denote the ratio of maximum required contacting forces in each force direction, we obtain a task ellipsoid A_β in the wrench space as

$$A_\beta = \left\{ (f_x, \cdots, \tau_z) \in R^6, \quad \frac{\tau_z^2}{r_1^2} + \frac{\tau_2^2}{r_2^2} + \frac{(f_x-c)^2}{r_3^2} + \frac{f_y^2}{r_4^2} + \frac{f_z^2}{r_5^2} + \frac{\tau_x^2}{r_6^2} \le \beta^2 \right\} \quad (21)$$

where the parameter $\beta \ge 0$, and the constant c denotes the offset of maximum required task force in the $+f_x$ direction with respect to $-f_x$. The shape of the task ellipsoid is determined by the force ratio $(r_i)_{i=1}^6$ and the constant c. The writing task requirement amounts to having relatively large values for r_1 and r_2.

The process of modeling a task by a task ellipsoid is quite complicated; it needs experience with the task and tasks of similar kinds. Observe the human action in learning a pencil

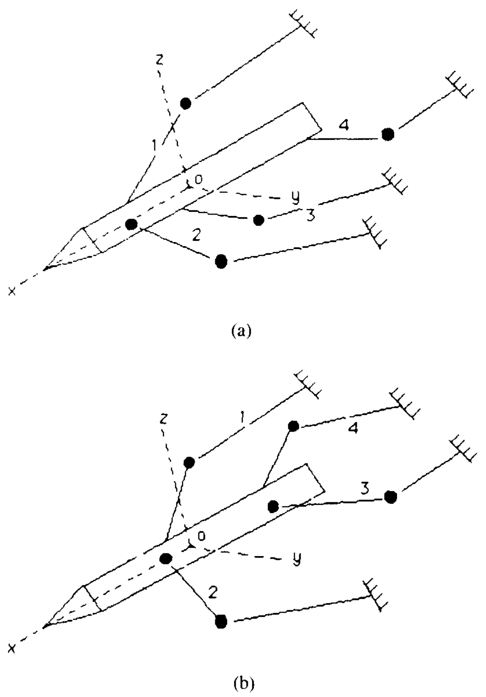

Fig. 5. Two grasp configurations to pencil.

grasping: initially, a child (with no previous experience) would probably grasp a pencil as shown in Fig. 5(b) to provide strong stability. However, since such a grasp does not provide much dexterity at the pencil lead, the child, when it grows up, will learn from its experience or is taught by adults to modify its task ellipsoid and gradually adapts its grasp of the pencil to the correct configuration in Fig. 5(a). This process is also manifested by a person's action in performing an unfamiliar task. It is only through trial and error that he learns to grasp the target object in the proper configuration [31]. It does take a great deal of modeling effort to specify a task ellipsoid for a specific task. Nevertheless, the difficulties can be reduced significantly as we could now store our "experience" on computers.

There are also other approaches to develop task ellipsoids. For example, if stiffness control is used for the hand, then the maximum expected positional uncertainties in each of the task directions may be used to scale the axes. Also, during parts mating, jamming can be avoided if certain constraints on the ratios of the contact forces are satisfied [29] using these constraints on the force ratios to scale the ellipsoid axis is another approach.

Generalizing from these examples, we will assume thereafter that our task is modeled by a task ellipsoid given in (22), where Q is a 6×6 positive definite symmetric matrix, and $a \in R^6$ reflects the asymmetry properties of the task. The definition of the ellipsoid A_β here is much more general than in the previous examples and is applicable to a large class of tasks. Our goal then is to construct a quality measure that accounts for this task requirement:

$$A_\beta = \{ y \in R^6, \langle y, Qy \rangle + \langle a, y \rangle \leq \beta^2 \}. \qquad (22)$$

2) Task-Oriented Quality Measure μ:

Definition 3: Given the task ellipsoid A_β in (22), we define the task-oriented quality measure $\mu(G)$ of a grasp G to be

$$\mu(G) = \sup \{ \beta \geq 0, \text{ such that } A_\beta \subset G(B_1^n \cap K) \} \qquad (23a)$$

when $a = 0$; i.e., it is the radius of the largest task ellipsoid that can be embedded in $G(B_1^n \cap K)$. If $a \neq 0$, the quality measure is defined by

$$\tilde{\mu}(G) = \sup \{ \alpha > 0 \text{ such that } A_\beta \subset G(B_{1/\alpha}^n \cap K) \} \qquad (23b)$$

where A_β is one of the sets in (22) that contains the origin in its interior.

We observe that the quality measure (23a) is the largest task ellipsoid that can be embedded in $G(B_1^n \cap K)$, and the quality measure (23b) is the inverse of the image of the largest ball intersected $\boldsymbol{K}$ which can cover an appropriate task ellipsoid. We require the task ellipsoid in the later definition to contain the origin in its interior to avoid degeneracy; namely, only stable grasps give nonzero quality measures. It is easy to show that when the task ellipsoid is centered at the origin, $K_1, K_2 > 0$ exist such that

$$K_1 \tilde{\mu}(G) \leq \mu(G) \leq K_2 \tilde{\mu}(G), \qquad \text{for all grasps } G. \quad (24)$$

Hence we may focus our attention in what follows to the form (23a).

A necessary and sufficient condition for a grasp $\boldsymbol{G}$ to be stable is $\mu(G) > 0$. Unlike the volume measure ν, we do not have unstable grasps with $\mu(G) > 0$. Let $F(B)$ denote the space of all grasps to an object $\boldsymbol{B}$. Then μ is a function

$$\mu: F(B) \rightarrow R_+ \qquad (25)$$

with the following properties: 1) it is positively homogeneous:

$$\mu(\lambda G) = \lambda \mu(G), \qquad \text{for all } \lambda \geq 0; \qquad (26)$$

2) it is bi-invariant:

$$\mu(G) = \mu(\tilde{T} G) \qquad (27a)$$

where $\tilde{T}$ is the body coordinate transformation, and

$$\mu(G) = \mu(\hat{T}_b G) \qquad (27b)$$

where $\hat{T}_b$ is the matrix that represents a change of the torque origin.

Proof: 1) We have the following:

$$\begin{aligned}
\mu(\lambda G) &= \sup \{ \beta \text{ such that } A_\beta \subset (\lambda G)(B_1^n \cap K) \} \\
&= \sup \left\{ \beta \text{ such that } \frac{1}{\lambda} A_\beta \subset G(B_1^n \cap K) \right\} \\
&= \sup \{ \beta \text{ such that } A_{(\beta/\lambda)} \subset G(B_1^n \cap K) \} \\
&= \sup \{ \lambda \beta' \text{ such that } A_{\beta'} \subset G(B_1^n \cap K) \} \\
&= \lambda \mu(G).
\end{aligned}$$

2) The proof follows from the definition since both the sets A_β and $G(B_1^n \cap K)$ are transformed by the same transformation matrices.

We have introduced three quality measures to guide the optimal selection of a grasp. The quality measures δ and ν are useful for simple tasks and for tasks in an unknown environment. These quality measures are easy to compute and are geometrically meaningful. The volume measure ν is invariant under both a body coordinate transformation and a change of the torque origin. In many applications this property is especially desirable as there is no natural choice of a body coordinate and a torque origin. The quality measure μ of this section is useful when the tasks involved are sophisticated.

We remark that the results of this section still hold when the tasks are modeled by other convex sets. This is important since not all tasks can be modeled by ellipsoids. Example 6 shows how the results are generalized to an arbitrary convex set.

Example 6: Consider a task modeled by an open convex set C centered at a point b in the wrench space of the object. We define from C a new set $\hat{C} = C - b = \{y - b, y \in C\}$ which is a translation of C to the origin and contains the origin in its interior. Choose a $\lambda_0 > 0$ so that $b + \lambda_0\hat{C}$ also contains the origin in its interior, and define a task quality μ_1 to be

$$\mu_1(G) = \sup \{\alpha, \text{ such that } (b + \lambda_0\hat{C}) \subset G(B^n_{1/\alpha} \cap K)\}. \tag{28}$$

It is easy to verify that the measure μ_1 has all the properties of the measure μ.

We conclude this section with a sketchy argument to show why using the task ellipsoid of (21) the grasp configuration in Fig. 5(a) will give higher quality than that in Fig. 5(b). First, the task ellipsoid is assumed to be long in the $\pm\tau_z$ and $\pm\tau_y$ directions, and the torque origin is at o; as we move fingers 1, 2, and 3 down to the pencil lead end, we increase the effective moment arm. Consequently, we can generate more useful task torques per unit contact force in the grasp of Fig. 5(a) than in the grasp of Fig. 5(b). This shows that grasp Fig. 5(a) is a superior grasp over the grasp Fig. 5(b) for this task.

D. Numerical Computations of Quality Measures

In this section, we use some elementary convex analysis to implement the numerical computations of the quality measures μ, δ, and ν. Proofs of some of the results here are standard in [13]. We first introduce the concept of a support function of a convex set $H \in R^n$.

Definition 4: Let $H \subset R^n$; the support function $\phi(\cdot|H)$: $R^n \to R$ of H is defined as

$$\phi(x|H) = \sup \{\langle x, \tilde{x}\rangle, \tilde{x} \in H\}. \tag{29}$$

Several properties of the support function of a convex set H in R^n are studied in [13]. We quote the following results.

Theorem 4: For any two closed convex sets H_1 and H_2 in R^n, $H_1 \subset H_2$ if and only if $\phi(x|H_1) \leq \phi(x|H_2)$ for all $x \in R^n$.

Proof: See [13, p. 113].

It follows that a closed convex set H can be expressed as the set of solutions to a system of inequalities given by its support function

$$H = \{\tilde{x}, \langle\tilde{x}, x\rangle \leq \phi(x|H), \text{ for all } x \in R^n\}. \tag{30}$$

Therefore, H is completely determined by its support function, and we have a one-to-one correspondence between closed convex sets in R^n and certain (support) functions in R^n.

The support function of a convex set, specified by a set of linear and quadratic inequality constraints, can be computed numerically by algorithms in [14]–[16]. Using the idea of support functions, we are now ready to compute the quality measure μ of (23): by Theorem 4, $A_\beta \subset G(B^n_1 \cap K)$ if and only if

$$\phi(x|A_\beta) \leq \phi(x|G(B^n_1 \cap K)), \text{ for all } x \in R^n. \tag{31}$$

However, the support function of an ellipsoidal convex set A_β is given (see [13, p. 120]) by

$$\phi(x|A_\beta) = \langle -Q^{-1}a, x\rangle + [2\sigma\langle x, Q^{-1}x\rangle]^{1/2} \tag{32}$$

where $\sigma = (1/2)\langle a, Q^{-1}a\rangle + \beta^2$.

On the other hand, the support function of $G(B^n_1 \cap K)$ is

$$\begin{aligned}\phi(y|G(B^n_1 \cap K)) &= \sup \{\langle y, \tilde{y}\rangle, \tilde{y} \in G(B^n_1 \cap K)\}\\ &= \sup \{\langle y, Gx\rangle, x \in (B^n_1 \cap K)\}\\ &= \sup \{\langle G^t y, x\rangle, x \in B^n_1 \cap K\}\\ &= \phi(G^t y|B^n_1 \cap K).\end{aligned} \tag{33}$$

Since the support function of the set $B^n_1 \cap K$ is readily computable using existing algorithms [15], the calculation of $\mu(\cdot)$ is straightforward by stepwise incrementing of β.

In [14] the author described an algorithm that found the nearest distance to a point of a polytope. The polytope may be specified by the convex hull of k points $(p_1, \cdots, p_k)$ in a n-dimensional space or by its support function. This algorithm is implemented in [15]. By repeatedly calling this subroutine, one could, in principle, compute the quality measures δ and ν. We outline here a procedure for calculating $\delta(G)$ together with a force domain K in R^n. Of course, this might not be the most efficient method, but it gives an idea on how the computations of these quality measures can actually be performed. First, one computes all $(n-1)$-dimensional faces of the set $G(B^n_1 \cap K)$ and denotes them by $G^c(B^n_1 \cap K)$ (see [25] also). Then, one computes for each face the distance of the face to the origin and denotes it by d_i. The minimum of these d_i is then the quality measure δ. The calculation of the volume measure ν can be done from its definition and the volume definition in a general n-dimensional space.

E. Optimal Grasp Selection

In this section we address the problem of maximizing the function $\mu(\cdot)$ over $F(B)$ subject to certain geometric and reachability constraints. For this purpose, we assume that we have 1) a full geometric description of the object in (34); i.e., it is given by a set of hyperplanes

$$\hat{h}_i(x, y, z, c_i) = 0, \qquad \text{for } i = \{1, \cdots, l\} \tag{34}$$

and 2) a complete model of the task or the task environment by

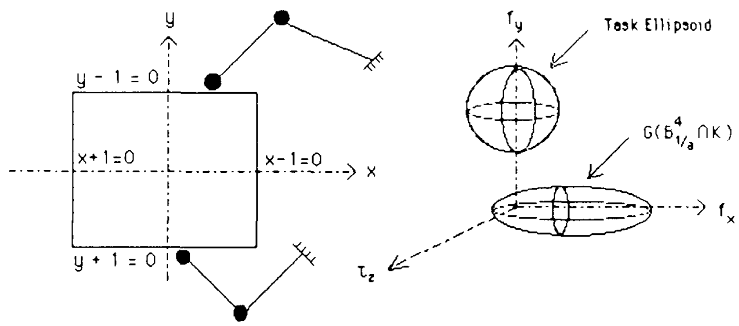

Fig. 6. Two-fingered planar grasp.

a task ellipsoid. We also assume that the object described by (34) has well-defined normals almost everywhere; i.e., the set where normals are not defined has an area of measure zero (e.g., the edges of a cube). Let contact point p_i of the ith fingertip ($i \in \{1, \cdots, k\}$) belong to contact surface $\hat{h}_{i_j}$ for some $i_j \in \{1, \cdots, l\}$; i.e., $\hat{h}_{i_j}(p_i, c_{i_j}) = 0$. Notice that the index i stands for the ith finger while the index i_j stands for the i_jth surface. Denote the unit normal to the contacting surface by $f_1^i(p_i)$, namely,

$$f_1^i(p_i) = \frac{\nabla h_{i_j}(p_i)}{\|\nabla h_{i_j}(p_i)\|}. \tag{35}$$

Also, let the two unit tangent vectors to h_{i_j} at p_i be $f_2^i(p_i)$ and $f_3^i(p_i)$, which determine, along with $f_1^i(p_i)$, an orthonormal basis at point p_i. Let $m_4^i(p_i) = f_1^i(p_i)$ denote a soft finger contact; we write explicitly the dependence of the grasp matrix $\boldsymbol{G}$ on the contact configuration $(p_i)_{i=1}^{i=k}$ as

$$G = \begin{bmatrix} f_1^1(p_1) & \cdots & f_3^1(p_1), & \cdots & f_3^k & 0 \\ f_1^1(p_1)\times(p_1-o) & \cdots & f_3^1(p_1)\times(p_1-o) & \cdots & f_3^k\times(p_k-o) & m_4^k(p_k) \end{bmatrix}. \tag{36}$$

The point p_i, $i = \{1, \cdots, k\}$, belongs to the surface h_{i_j}, and consequently, it satisfies one of the (34) constraints. By composing the function $\boldsymbol{G}$ with μ, we obtain a new function $\bar{\mu}$: $R^{3k} \to R$ from the parameter space $p_i = (p_x^i, p_y^i, p_z^i)$, $i = \{1, \cdots, k\}$ into the reals R given by $\bar{\mu} = \mu(G)$. The problem of optimal grasping is then the problem of

$$\underset{\{(p_i,\cdots,p_k)\in R^{3k}, h_{i_j}(p_i,c_{i_j})=0\}}{\text{maximize}} \quad \bar{\mu}(p_1, p_2, p_3, \cdots, p_k), \tag{37}$$

a constrained optimization problem.

The function $\bar{\mu}$ may be nondifferentiable with respect to its argument $p_i = (p_x^i, p_y^i, p_z^i)$, and is often called a nondifferentiable optimization problem. The computation involved is usually heavy, but efficient algorithms are being developed in the literature [16].

Example 7: We conclude this section with an example of a two-fingered grasp to a rectangular planar object. The object shown in Fig. 6 has weight c and is given by the four hyperplanes (i.e., lines) in R^2. Let

$$h = h(x, y) = 0 \tag{38}$$

be the line equations. We assume that the task ellipsoid is a ball in R^3, i.e.,

$$A_\beta = \{(f_x, f_y, \tau_z) \in R^3, f_x^2 + (f_y - c)^2 + \tau_z^2 \le \beta^2\}. \tag{39}$$

We intend to find a grasp that is optimal with respect to the task. The unit normal $f_1^i(p_i)$ and the unit tangent vector $f_2^i(p_i)$ to (38) at p_i, $i = \{1, 2\}$, are given by

$$f_1^i(p_i) = \frac{\nabla h(p_i)}{\|\nabla h(p_i)\|} = \nabla \tilde{h}(p_i) = \begin{pmatrix} \dfrac{\partial \tilde{h}(p_i)}{\partial x} \\ \dfrac{\partial \tilde{h}(p_i)}{\partial y} \end{pmatrix}$$

$$f_2^i(p_i) = \begin{pmatrix} \dfrac{\partial \tilde{h}(p_i)}{\partial y} \\ \dfrac{\partial \tilde{h}(p_i)}{\partial x} \end{pmatrix} \tag{40}$$

where the symbol "$\tilde{\ }$" denotes normalized quantities.

We observe that the tangent and the normal vectors to the object are well defined everywhere except at the corners which we shall not consider. The resulting torques of $f_1^i(p_i)$ and $f_2^i(p_i)$ about the origin are

$$m_1^i(p_i) = p_y^i \frac{\partial \tilde{h}(p_i)}{\partial x} - p_x^i \frac{\partial \tilde{h}(p_i)}{\partial y}$$

$$m_2^i(p_i) = p_y^i \frac{\partial \tilde{h}(p_i)}{\partial y} + p_x^i \frac{\partial \tilde{h}(p_i)}{\partial x}. \tag{41}$$

Assuming point contacts with friction, we obtain the grasp matrix $\boldsymbol{G}$:$R^4 \to R^3$:

$$G = \begin{bmatrix} f_1^1(p_1) & f_2^1(p_1) & f_1^2(p_2) & f_2^2(p_2) \\ m_1^1(p_1) & m_2^1(p_1) & m_1^2(p_2) & m_2^2(p_2) \end{bmatrix}, \tag{42}$$

and the force domain $\boldsymbol{K} \in R^4$:

$$K = \{x \in R^4, x_1 \ge 0, x_2^2 \le \mu_1^2 x_1^2, x_3 \ge 0, x_4^2 \le \mu_2^2 x_x^2\}. \tag{43}$$

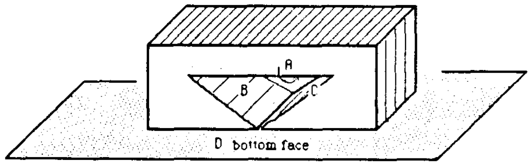

Fig. 7. Oddly shaped object on table.

Observe that to balance any external wrench $(f_x, f_y, t_z)^t$, the applied finger force $x \in R^4$ must satisfy

$$\begin{bmatrix} f_x \\ f_y \\ \tau_z \end{bmatrix} = G \begin{bmatrix} x_1 \\ x_2 \\ x_3 \\ x_4 \end{bmatrix}. \tag{44}$$

If we can find such an x in K that solves (44), then static equilibrium is possible. For example, when $(f_x, f_y, \tau_z) = (0, c, 0)$, one solution would be $p_1 = (0, -1)$, $p_2 = (0, 1)$, $x_i = 0$ for $i > 1$, and

$$x_1 = c \left\{ \frac{\partial \tilde{h}(p_1)}{\partial y} \right\}^{-1}.$$

The solution of (37) for the two-dimensional example is still computationally intensive, yet a qualitative description of the set $G(B^4_{1/\alpha} \cap K)$ can be given. Apparently, the contact point (p_1, p_2) must not lie on the same edge to achieve a stable grasp. The four candidate grasps left are

1) $p_1 = (0, -1)$, $p_2 = (0, 1)$

2) $p_1 = (1, 0)$, $p_2 = (-1, 0)$

3) $p_1 = (0, -1)$, $p_2 = (-1, 0)$

4) $p_1 = (0, 1)$, $p_2 = (1, 0)$. (45)

Since the task ellipsoid is located right above the f_y axis, a "good" grasp should have the set $G(B^4_1 \cap K)$ oriented along the f_y direction. Any grasps with $G(B^4_1 \cap K)$ oriented along other directions are considered as inefficients grasps. The last two pairs of grasps do not give good grasp qualities because $G(B^4_1 \cap K)$ in these cases are not oriented along the f_y direction, and neither does grasp 2). It is only true for grasp 1); consequently, it gives higher quality μ than any other grasps. Notice that the differences between grasps 1) and 2) are becoming insignificant as weight of the object is reduced.

1) Additional Constraints and Dynamic Grasping: Additional constraints, besides the geometric constraints to be considered, are *reachability constraints* and *hand constraints.* Reachability constraints as considered in [10] include accessibility of the hand to the target object and obstacles in the working environment. For example, when an oddly shaped object shown in Fig. 7 resides on the top of a table, its faces A, B, C, and D are not accessible by a robot hand.

While constraints on faces A, B, and C could be classified as intrinsic constraints, the constraint on face D is extrinsic and could be eliminated if we turn the object around (and create new constraints). There are also other types of constraints dependent upon the environment and the object shape. See [10] for further discussions of reachability constraints.

Hand constraints often refer to constraints imposed by geometry, working volume of the hand, and spreading distances of each finger. Suppose that, in addition to the k constraints of the previous section, we have p reachability constraints and $\tilde{p}$ hand constraints; then to determine the optimal grasp, we need to solve the optimization problem (37) subject to a total of $(k + p + \tilde{p})$ constraints.

Recent advances in dextrous hand design [23] enable fine motion of the object within the robot hand [6], [7]. Therefore, the extrinsic reachability constraints may be eliminated by performing fine motions of the object in the hand. For example, as in Fig. 7, while the face D is not reachable in the initial grasp configuration it becomes reachable once the object is picked up from the table and a better grasp configuration may be obtained. Human hands perform such operations frequently; when one grasps a pencil, one would first pick up the pencil and then manipulate it around in the hand to get to the final grasp configuration which is the global optimum.

In addition, we can see that the quality measure μ computed depends heavily on the specific task to be performed. When the task varies, the measure of the grasp may change. A grasp which is optimal for one task may be totally different for another. The process of updating the grasp in response to a changed task ellipsoid is called dynamic grasping. Dynamic grasping happens on many occasions. When a cup is filling with water, the weight of the cup increases with time and the task ellipsoid varies. We observe that the corresponding action of the human hand is to move up the finger so as to keep the grasp optimal. When a target object in compliant motion is moved from one environment to another, the ratio of maximum expected collision forces changes and updating the original grasp becomes necessary to carry out the task.

IV. Suggestions for Future Work

We have studied in the paper the problem of optimal grasping by a multifingered robot hand. The optimality criteria are based on some quality measures defined in Section III. As all these measures are numerically computable, the problem has feasible solutions. Part of our future work is to study the numerical issues in greater detail to provide a complete solution to the problem.

The grasp quality measures considered in the paper are in the force domain. A dual approach would be through the velocity domain or a combination of both the force and the velocity domains. As the velocity domain attributes of a grasp represent dexterity in effecting motion, a large grasp quality in the velocity domain means large motion of the object can be achieved with just small motion of the fingertips. Refining the quality measures to include velocity domain attributes can be a topic of future work. Also, it is important to extend our work to include hand kinematics, i.e., structures of each finger, in the grasp quality measures.

In the paper, the assumption of one contact per finger at the finger tip is very strict and impractical. Very often, a human relies on contacts (point or area contact) at finger links and at the hand palm as well to achieve a *good* grasp. As a contact with finite area can be approximated by many point contacts, one usually chooses a small number of contacts in a grasp (a precision grasp) to grasp a light object and a large number of contacts in a grasp (a power grasp) to grasp a heavy object. In this regard, the dimension of the force domain $\boldsymbol{K}$ is an optimization variable as well. We need to choose a grasp that is optimal not only with respect to the contacting locations but also to the number of contacts. Namely, we need to answer the following questions: given two grasps,

$$G_1: R^{12} \rightarrow T_m^* M \tag{46}$$

$$G_2: R^{36} \rightarrow T_m^* M \tag{47}$$

with associated force domains $K_1 \subset R^{12}$ and $K_2 \subset R^{36}$ and a common task to be performed, how do we compare their relative qualities? Consider again the pencil grasping example. Suppose that G_1 corresponds to a regular human dextrous grasp with four contacts, and G_2 is a power grasp with 12 contacts. Apparently, it might be true that $\mu(G_2) \geq \mu(G_1)$, but a human always selects grasp G_1 because it gives not only better manipulatability but also better sensitivity. On the other hand, if the pencil is replaced with a Chinese brush pen (usually heavy and large), then the grasp G_2 might be chosen instead.

The theory developed so far is still not adequate to answer the question of how physical properties (weight, shape, size, etc.) of an object and task requirement determine not only the grasping locations but also the *number of contacts of a grasp*. However, it does present some useful approaches to the problem.

Acknowledgment

We would like to thank Dr. Robyn Owens, Dr. Brad Paden, and John Hauser, Paul Jacobs, and Greg Heinzinger for their critical and useful comments. We also like to thank the reviewers and Yu Wang for several useful suggestions during the revision.

References

[1] M. Brady, *et al., Robot Motion Planning and Control.* Cambridge, MA: MIT Press, 1983.
[2] R. Paul, *Robot Manipulators: Mathematics, Programming, and Control.* Cambridge, MA: MIT Press, 1981.
[3] H. Hanafusa and H. Asada, "Stable prehension by a robot hand with elastic fingers," in *Proc. 7th ISIR,* Tokyo, Japan, 1977, pp. 361–368.
[4] H. Asada, "A robotic hand with elastic fingers and its application to assembly process," in *Proc. IFAC Symp. Information Control Problem in Production Engineering,* 1977, pp. 127–138.
[5] J. K. Salisbury, "Kinematic and force analysis of articulated hand," Ph.D. dissertation, Stanford Univ., Stanford, CA, Dept. of Mechanical Eng., May 1982.
[6] M. R. Cutkosky, "Grasping and fine manipulation for automated manufacturing," Ph.D. dissertation, Carnegie-Mellon Univ., Pittsburgh, PA, Dept. of Mechanical Eng., Jan. 1985.
[7] J. Kerr, "Analysis of multifingered hand," Ph.D. dissertation, Stanford Univ., Stanford, CA, Dept. of Mech. Eng., Dec. 1984.
[8] W. Holzman and J. M. McCarthy, "Computing the friction forces associated with a three-fingered hand," *IEEE J. Robotics, Automation,* vol. RA-1, pp. 206–210, Dec. 1985.
[9] J. Jameson, "Analytic techniques of automated grasp," Ph.D. dissertation, Stanford Univ., Stanford, CA, Dept. of Mech. Eng., June, 1985.
[10] T. Lozano-Perez, "Task planning," in *Robot Motion Planning and Control.* Cambridge, MA: MIT Press, 1982, pp. 473–498.
[11] O. Bottema and B. Roth, *Theoretical Kinematics.* New York: North-Holland, 1979.
[12] B. Paden, "Kinematics and control of robot manipulators," Ph.D. dissertation, Univ. of California, Berkeley, Dept. of EECS, Dec. 1985.
[13] R. T. Rockafellar, *Convex Analysis.* Princeton Mathematics Series, vol. 28. Princeton, NJ: Princeton Univ. Press, 1970.
[14] P. Wolfe, "Finding the nearest point in a polytope," *Mathematical Programming,* 1976, pp. 128–149.
[15] J. Hauser, "Proximity algorithms: Implementation and applications," Univ. of California, Berkeley, ERL Memo. UCB/ERL M86/53, May 1986.
[16] E. Polak, *Computational Methods in Optimization.* New York: Academic, 1971.
[17] W. Boothby, *An Introduction to Differentiable Manifolds and Riemannian Geometry.* New York: Academic, 1975.
[18] R. Abraham and J. Marsden, *Foundations of Mechanics.* 2nd ed. Menlo Park, CA: Benjamin/Cummings, 1978.
[19] J. D. Wolter, R. A. Volz, and A. C. Woo, "Automatic generation of gripping position," *IEEE Trans. Syst., Man, Cybern.*, vol. SMC-15, no. 2, pp. 204–213, Mar./Apr. 1985.
[20] J. Barber *et al.,* "Automatic two-fingered grip selection," in *Proc. IEEE Int. Conf. Robotics and Automation,* Apr. 1986, pp. 890–896.
[21] M. Peshkin and A. Sanderson, "Reachable grasps on a polygon: The convex rope algorithms," *IEEE J. Robotics, Automation,* vol. RA-2, no. 1, Mar. 1986.
[22] J. Loncaric, "Geometrical analysis of compliant mechanisms in robotics," Ph.D. dissertation, Harvard Univ., Cambridge, MA, Division of Applied Sciences, May 1985.
[23] S. C. Jacobsen, J. E. Wood, D. F. Knutti, and K. B. Biggers, "The Utah/MIT Hand: Work in progress," in *Robotics Research,* M. Brady and R. Paul, Eds. Cambridge, MA: MIT Press, 1984.
[24] H. Goldstein, *Classic Mechanics,* 2nd ed. Reading, MA: Addison-Wesley, 1980.
[25] T. Yoshikawa, "Manipulability of robotic mechanism," Kyoto Univ., Uji, Kyoto 611, Japan, Tech. Rep.
[26] Z. X. Li and S. S. Sastry, "Task oriented optimal grasping by multifingered robot hands," Univ. of California, Berkeley, ERL Memo. UCB/ERL M86/43, May 1986.
[27] ——, "Hybrid velocity/force control of robot manipulators: Stability and robustness," Univ. of California, Berkeley, ERL Memo., Jan. 1987.
[28] J. Kerr and B. Roth, "Special grasping configurations with dexterous robot hands," in *Proc. IEEE Int. Conf. Robotics and Automation,* Apr. 1986, pp. 1361–1367.
[29] D. E. Whitney, "Quasi static assembly of compliantly supported rigid parts," *J. Dynamic Syst., Meas., Contr.*, vol. 104, pp. 65–77, Mar. 1982.
[30] F. M. Callier and C. A. Desoer, *Multivariable Feedback Systems.* New York: Springer-Verlag, 1982.
[31] J. A. Kelso and J. E. Clark, *The Development of Movement Control and Co-ordination.* New York: Wiley, 1982.
[32] P. Jacobs, Research Seminar, Univ. of California, Berkeley, Apr. 1985.

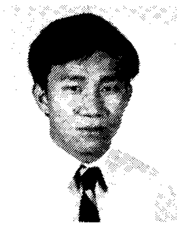

Zexiang Li was born in Hunan, China, in September 1961. He attended the Central-South Institute of Metallurgy, China, in 1978, and received the B.S. degree (with honors) in economics and electrical engineering from Carnegie-Mellon University, Pittsburgh, PA, in 1983, and the M.S. degree in electrical engineering and computer science (EECS) from the University of California, Berkeley, in 1985. He is currently completing the Ph.D. degree in the EECS Department, University of California at Berkeley.

In the summer of 1980 he worked in the Design Division at ALCOA, and in the summer of 1985 in the Legged Laboratory at Carnegie-Mellon University. His research interests include geometrical control theory, dynamics, kinematics, and control of robotic systems.

Mr. Li held the ALCOA Foundation Fellowship from 1979 to 1983 and the Early Anthory Fellowship from 1983 to 1984.

S. Shankar Sastry (S'79–M'80) received the B.Tech. degree from the Indian Institute of Technology, India, in 1977, the M.S. and Ph.D. degrees in electrical engineering in 1979 and 1981, respectively, and the M.A. degree in mathematics in 1980, all from the University of California, Berkeley.

After having been on the faculty of the Massachusetts Institute of Technology, Cambridge, from 1980 to 1982, he is currently an Associate Professor in the Electronics Research Laboratory, University of California, Berkeley. His areas of research interest are nonlinear circuits and systems, adaptive control, kinematics, and control of robots, intelligent rule-based control, and neural networks.

Dr. Sastry is an Associate Editor of the IEEE TRANSACTIONS ON AUTOMATIC CONTROL and is an Associate Editor of the *IMA Journal of Control and Information and Large Scale Systems.* He received the President of India Gold Medal in 1977, the IBM Faculty Development Award for 1983–1985, and the Presidential Young Investigator Award in 1985.